Combining Enhanced Competitive Code with Compacted ST for 3D Palmprint Recognition

Lunke Fei, Shaohua Teng, Jigang Wu
School of Computer Science and Technology,
Guangdong University of Technology
Guangzhou, China
flksxm@126.com,shteng@gdut.edu.cn,asjgwucn@outlook.com

Yong Xu, Jie Wen, Chunwei Tian
Shenzhen Graduate School,
Harbin Institute of Technology
Shenzhen, China
yongxu@ymail.com,wenjie@hrbeu.edu.cn,
chunweitian@163.com

***Abstract*—As one of important biometric traits, three dimensional (3D) palmprint has recently drawn considerable research interest in the field of palmprint-based authentication. Because 3D palmprint images have rich depth information and are difficult to be counterfeited. In this paper, a novel enhanced competitive code (Ecomp) is proposed to effectively represent the orientation features of palmprint by emphasizing the significance of the orientation, and a simple and effective compact-surface-type (cST) is used to describe the surface structures of 3D palmprint. The addition and multiplication schemes are respectively proposed to effectively combine the Ecomp and cST maps, and the proposed descriptors can better represent not only the 2D orientation but also the 3D surface shapes of the 3D palmprint. Experimental results on the widely used 3D palmprint database are presented to demonstrate the effectiveness of the proposed method on both 3D palmprint verification and identification.**

***Keywords*-Biometrics; 3D palmprint recognition; enhanced competitive code; compact ST;**

I. Introduction

As a biometric trait, palmprint mainly refers to the skin patterns on the inner palm surface. A palmprint contains many stable and discriminative features, including not only principal lines, wrinkles and textures but also rich minutiae and ridge features, which are considered to be immutable, permanent, and unique to a subject [1][2][3]. Thus, palmprint-based authentication is able to achieve reliable and desirable performance.

So far, many methods based on various kinds of palmprint features have been proposed for palmprint recognition. Typically, Zhang et al. [4] invented an online palmprint identification system by extracting a special orientation feature of palmprint, named as palmcode, which achieved quite good performance in a real time application. Inspired by the palmcode method, various orientation-based methods for palmprint recognition were proposed [3][5]. In addition, the scale invariant feature transform (SIFT) points were widely used for contactless palmprint recognition [6]. Minutiae and ridge-based features were generally extracted from high-resolution palmprint image (500 ppi) for forensic applications [7][8].

It is seen that the existing research mainly focus on two-dimensional (2D) palmprint image recognition. Quite recently, three-dimensional (3D) palmprint recognition has been receiving increasing research concerns. A 3D palmprint image has rich depth information, thereby it shows high robustness to illumination variations. Furthermore, a 3D palmprint image is hard to be counterfeited. Zhang et al. [9] designed a 3D palmprint data acquisition device with using structured light technology in 2008, by which they established a 3D palmprint database containing 8000 3D palmprint range data of 400 palms. Since then, various methods have been proposed for 3D palmprint recognition. Zhang et al. [10] binarized mean curvature image (MCI), Gaussian curvature image (GCI) and surface type (ST) of 3D palmprint into binary maps and fused them in matching score level. Meanwhile, the binarization operation loses much of the texture information existing in the MCI. In [11][12], Li et al. extracted both competitive code and line features from MCI and fused them at eithers core level or feature level achieving acceptable performance. Furthermore, Yang et al. [13] introduced the shape index representation to describe the geometry feature of 3D palmprint. Zhang et al. [14] formed a feature vector by using the block histogram of ST and used the collaborative representation (CR) to perform 3D palmprint identification achieving impressive performance.

In this paper, we propose a novel 3D palmprint recognition method in which more accurate dominant orientation and global statistic features are exploited and fused to provide more discriminative and robust information. The main contributions of this work are as follows. First, a novel enhanced competitive code method is proposed that captures the most dominant orientation of palmprint and meanwhile highlights the significance of the orientation feature. Second, a novel and effective compact-ST is used to describe the surface structure of 3D palmprint. Third, the enhanced competitive code and compact ST are effectively fused using addition and multiplication schemes. The proposed descriptors can not only better capture the orientation feature but also effectively preserve the structure characteristics of 3D palmprint. Forth, a series of experiments are conducted to evaluate the performance of the proposed method. To our knowledge, the proposed method can achieve the highest accuracy of palmprint recognition on the PolyU 3D palmprint database.

The remainder of this paper is organized as follows. Section II briefly review the curvature calculation of 3D palmprint. Section III proposes a 3D palmprint representation and recognition method by combining the enhanced competitive code and compact ST based features. Section

2327-0985/17 $31.00 © 2017 IEEE
DOI 10.1109/ACPR.2017.62

IV presents experimental results, and Section V offers the conclusion of this paper.

II. Related works

In this section, we briefly review the the mean and Gaussian curvatures of 3D palmprint images. 3D palmprint can be considered as a surface with various convex and concave structures. The mean and Gaussian curvature are two intrinsic measures of a 3D surface for they depend only on the surface shape but not on the way how the surface is placed in the data acquisition [10]. Thus, we obtain the mean and Gaussian curvatures of 3D palmprint before feature extraction. The mean curvature (H) and Gaussian curvature (K) can be obtained from the 3D palmprint data as follows [9]:

$$H = \frac{(1+f_x^2)f_{xy} + (1+f_y^2)f_{xx} - 2f_x f_y f_{xy}}{2(1+f_x^2+f_y^2)^{3/2}}, \quad (1)$$

$$K = \frac{f_{xx}f_{yy} + f_{xy}^2}{(1+f_x^2 f_y^2)^2}, \quad (2)$$

where f is the depth of a point in the 3D palmprint ROI, $f_x(f_y)$, $f_{xx}(f_{yy}, f_{xy})$ are the first order and second order partial derivatives of f to $x(y)$ coordinate, respectively.

The curvatures H and K can be directly calculated by convolving images with various predefined window templates [**?**]. The partial derivative estimation window templates are defined as $D_x = d_0 d_1^T$, $D_y = d_1 d_0^T$, $D_{xx} = d_0 d_2^T$, $D_{yy} = d_2 d_0^T$ and $D_{xy} = d_1 d_1^T$ respectively, where column vectors $d_i (i = 0, 1, 2)$ are given as: $d_0 = \frac{1}{7}[1\ 1\ 1\ 1\ 1\ 1\ 1]^T$, $d_1 = \frac{1}{28}[-3\ -2\ -1\ 0\ 1\ 2\ 3]^T$ and $d_2 = \frac{1}{84}[5\ 0\ -3\ -4\ -3\ 0\ 5]^T$. Specifically, before curvature calculation, the range data of 3D palmprint ROI is smoothed by using a binomial filter $S = ss^T$, where s is a column vector defined as $s = \frac{1}{64}[1\ 6\ 15\ 20\ 15\ 6\ 1]^T$. Therefore, the partial derivative maps of the 3D palmprint $f(x, y)$ in (1) and (2) can be easily calculated using

$$f_u(x, y) = D_u * S * f_u(x, y), (u = x, y, xx, yy, xy). \quad (3)$$

III. Enhanced competitive code and compact ST

In this section, an enhanced competitive code method is proposed to represent the orientation features of 3D palmprint, and a simple and compact surface type is used to describe the surface shape of 3D palmprint. Then, the enhanced competitive code and compact ST are combined in two ways for 3D palmprint representation and recognition.

A. Enhanced competitive code

To facilitate the orientation feature extraction, we transform the mean curvature data into gray-scale image, namely MCI. The detailed conversion can be found in [8]. Figure 1 (b) shows an example of the MCI obtained from a 3D palmprint. It is seen that the MCI can better reflect the line features of the 3D palmprint image. The following orientation feature extraction of palmprint is essentially based on the MCI of 3D palmprint.

The competitive code is one of popular orientation representation methods that can extract the most dominant orientation of palmprint. Particularly, it uses the real parts of six Gabor filters with orientations of $j\pi/6 (j = 0, 1, ..., 5)$ to obtain the dominant orientation of a palmprint based on the winner-take-all principle. The real part of the Gabor filter has the following general form:

$$G(x, y, \theta, \mu, \sigma, \beta) = \frac{1}{2\pi\sigma\beta} exp(-(\frac{x^2}{\sigma^2} + \frac{y^2}{\beta^2})) \\ cos(2\pi\mu(xcos\theta + ysin\theta)), \quad (4)$$

where μ is the radial frequency in radians per unit length, θ is the orientation of the Gabor function in radians, and σ and β are the standard deviations of the elliptical Gaussian along the x and y axis, respectively. The optimal parameter setting can be found in [4]. In dominant orientation feature extraction, six Gabor filters are convolved with the MCI. The orientation of the Gabor filter having the maximum filter response with the MCI is treated as the dominant orientation, the index of which is used as the competitive code. Suppose that G_j is the G with orientation of $j\pi/6 (j = 0, 1, ..., 5)$, the extraction of the competitive code can be represented as:

$$r_j(x, y) = G_j \otimes I(x, y), \quad (5)$$

$$Comp(x, y) = arg \max_j r_j(x, y), \quad (6)$$

where $I(x, y)$ is the MCI, "$\otimes$" is the convolution operator and $Comp(x, y)$ represents the competitive code.

It is known that the competitive code is determined based on the principle that the filter response will reach maximum when the Gabor filter orientation is consistent with the line orientation of the palmprint. In the MCI of a 3D palmprint image, pixels in principal lines and wrinkles have obvious and stable orientation features. By contrast, some pixels in the flat area of palmprint usually have no obvious orientation feature. In other words, the competitive codes can represent the dominant orientation feature of the pixels in palmprint lines. Nevertheless, the competitive code obtained using winner-take-all rule may not precisely represent the dominant orientation feature of the pixels in the flat area having no obvious dominant orientations.

According to the theory of competitive code extraction, the maximum filter responses of the pixels in some palmprint lines are usually greater than those of the pixels in the flat area of the palmprint. Therefore, the magnitude of the maximum filter response of a point can represent the significance of the dominant orientation. Following this experience, we use the relationship among the maximum filter responses to determine the confidence of the competitive code. Given a MCI, the maximum filter response of palmprint image $I(x, y)$ with Gabor filters is denoted by $r_{max}(x, y)$, and can be obtained by:

$$r_{max}(x, y) = arg \max_r r_j(x, y). \quad (7)$$

(a) (b) (c) (d) (e)

Figure 1. The MCI, competitive code map, confidence mask and Ecomp map of a 3D palmprint. (a) A 3D palmprint image; (b) The MCI of the 3D palmprint; (c) The competitive code map of the MCI; (d) The confidence mask, and (e) the Ecomp map.

Then, we can define a threshold T to estimate the confidence of a competitive code by thresholding r_{max} and thus use a mask M to locate the confidence information of the competitive code as follows:

$$M(x,y) = \begin{cases} 1 & \text{if } r_{max}(x,y) \geq T \\ 0 & \text{else.} \end{cases} \quad (8)$$

Intuitively, threshold T should be adaptive to different palms. So the following scheme is used to determine T. We sort the magnitude of r_{max} to identify q percent of pixels as the significant ones. Particularly, the codes with the largest 40% magnitudes of r_{max} are treated as the significant competitive codes.

Based on the competitive code of palmprint and corresponding orientation confidence, an enhanced competitive code method (Ecomp) can be defined as follows:

$$Ecomp(x,y) = 2{\times}Comp(x,y) - M(x,y). \quad (9)$$

It is seen that the Ecomp uses double orientation codes of the competitive code method to better represent orientation feature of palmprint. Figure 1 shows the competitive code and enhanced competitive code maps of a 3D palmprint.

B. Local descriptor of combining Ecomp with cST

A 3D image essentially consists of various convex and concave surfaces, and eight fundamental surface types (ST) [9][14] can be defined to describe structures of these surfaces corresponding to eight fundamental shapes, which are illustrated in Table I, where H and K are the mean and Gaussian curvatures, respectively.

Table I
ST DEFINITION BASED ON THE SIGNS OF THE MEAN AND GAUSSIAN CURVATURES.

	K>0	K=0	K<0
H<0	Peak(ST=1)	Ridge(ST=2)	Saddle Ridge(ST=3)
H=0	None(ST=4)	Flat(ST=5)	Minimal Surface(ST=6)
H>0	Pit(ST=7)	Valley(ST=8)	Saddle Valley(ST=9)

The mean and Gaussian curvature of 3D palmprint obtained using (1) and (2) are usually float. To effectively classify the points in a 3D palmprint image into nine STs, the scales of H and K are usually quantized to determine the intervals to define the cases of H=0 and K=0, respectively, which can be simply implemented by defining two thresholding parameters ε_H and ε_K. For example, in [14], both parameters are empirically set as ε_H=0.03 and ε_K=0.015, respectively.

ST generally reflect the surface structures of 3D palmprint. However, in practical calculation of ST, H and K are generally float value, and therefore it is difficult to define the reasonable intervals of H=0 and K=0. Further, there is no real surface corresponding to the type of H=0 and K >0. Therefore, we use a simple compact-ST (cST) without considering the scenarios of H=0 and K=0 to represent the surface type features of 3D palmprint. The cST is defined as in Table II. It is seen that the cST only depends on the positive and negative signs of curvatures, which is suitable for the float number calculation. So the cST is quite effective and shows much robust to the small variations of curvatures than the ST.

Table II
COMPACT ST.

	K<0	K>0
H<0	cST=1	cST=2
H>0	cST=3	cST=4

In general, the Ecomp can accurately represent 2D orientation features of a 3D palmprint, and cST can robustly reflect the 3D structure characteristics of the 3D palmprint. Therefore, combining the Ecomp with cST can effectively represent both the 2D and 3D features of a 3D palmprint. It is seen that different areas of a 3D palmprint have different line, texture and structure characteristics. So we propose to use block-wise based descriptors of 2D Ecomp and 3D cST features to represent the 3D palmprint. Specifically, two schemes based on addition and multiplication are respectively designed to combine the Ecomp with cST.

Ecomp Adds cST: Given a 3D palmprint, we first calculate the Ecomp and cST features of the palmprint. Then, we uniformly divide the feature maps, including the Ecomp and cST feature maps, into a set of $p{\times}p$ non-overlapping blocks, and the block size is empirically set to $16{\times}16$ pixels. For each block, we calculate the histogram of the Ecomp and cST, and further concatenate the block-wise Ecomp and cST histogram, respectively. Finally, the Ecomp and cST histogram of the palmprint are directly concatenated, and we call the descriptor of Ecomp adding cST as ECST_A.

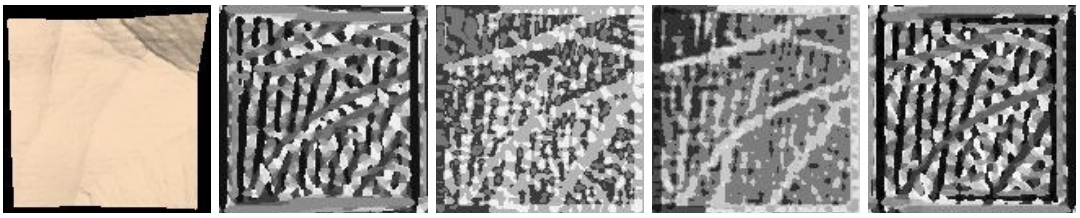

(a) (b) (c) (d) (e)

Figure 2. Feature maps of a 3D palmprint. (a) A 3D pamprint image; (b) The Ecomp map; (c) The ST map; (d) The cST map, and (e) the Ecomp_cST map of the palmprint.

Ecomp Multiplies cST: Ecomp and cST respectively represent the 2D orientation and 3D surface shape features of 3D palmprint. It is seen that the orientation and shape features are heavily associated. For example, a point of a 3D palmprint with a obvious orientation feature usually has high curvatures. Hence, a simple and effective multiplication scheme can be defined to combine the Ecomp with cST as follows:

$$Ecomp\_cST(x,y) = (Ecomp(x,y)-1)\times 4 + cST(x,y). \tag{10}$$

where 4 means the basic type number of cST. Therefore, the Ecomp_cST contains both the 2D orientation and 3D surface structure features of a 3D palmprint. Figure 2 shows an Ecomp_cST map of a 3D palmprint image. Then, the similar block-wise based Ecomp_cST descriptor can be formed and named as ECST_M.

C. ECST based 3D palmprint recognition

The Chi-square distance [15], that is χ^2-divergence, can be used to measure the dissimilarity between two ECST descriptors:

$$\chi^2(u,v) = \sum_{i}^{m} \frac{(u_i - v_i)^2}{u_i + v_i}, \tag{11}$$

where u and v are two histograms with m bins and $u_i(v_i)$ is the statistic at $i-th$ bin. Therefore, we can measure the similarity between two 3D palmprint images based on the Chi-square distance of the ECST based descriptors, and a small Chi-square distance represents a high similarity.

IV. Experiments

In this section, we conduct both palmprint verification and identification to evaluate the performance of the proposed method.

A. 3D palmprint database

The PolyU 3D palmprint database contains 8,000 3D palmprint images collected from 200 individuals, and 20 palmprint images were captured from both the left and right palm for each individual. In total, there are 400 palms of palmprint images and each palm has 20 samples. The region of interest (ROI) of the 3D palmprint image with the sizes of 128×128 pixels are also available in the database. Figure 3 shows some typical 3D palmprint images of the PolyU database.

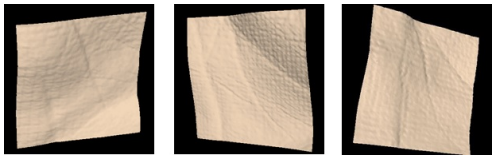

Figure 3. Three typical 3D palmprint images of the PolyU database.

B. Palmprint verification

Palmprint verification is one-to-one comparison to determine whether two compared palmprint images are from the same palm or not. A match is called as a genuine (or successful) match if both palmprint images are from the same palm, and otherwise the match is counted as an impostor (or unsuccessful) match [4]. In our palmprint verification experiments, each sample will be matched with all other samples in the PolyU database. False Acceptance Rate (FAR) and Genuine Acceptance Rate (GAR) are used to evaluate the verification performance of the proposed method. The Receiver Operating Characteristic (ROC) curve, which is a graph of FAR versus GAR for all possible decision thresholds, of the proposed method is drawn and shown as in Figure 4.

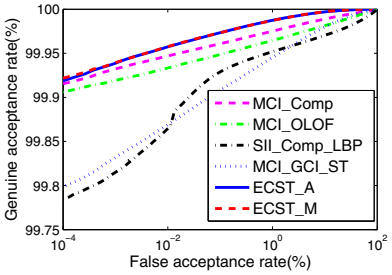

Figure 4. The ROC curves of palmprint verification obtained using different methods.

Further, the conventional representative 3D palmprint recognition methods are implemented to compare the performance of our method. They are MCI competitive code fusing with location method (referred to as MCI_Comp) [11], MCI ordinal code method (referred to as MCI_OLOF) [16], SII orientation feature fused with SII LBP method (referred to as SII_Comp_LBP) [13], and MCI, GCI and ST binarization and fusion method (referred to as MCI_GCI_ST) [10]. The ROC curves obtained by using these baseline methods are also shown in Figure 4.

Table IV
THE ACCURACY (%) OF PALMPRINT IDENTIFICATION OBTAINED BY USING DIFFERENT METHODS ON THE POLYU 3D PALMPRINT DATABASE.

#n	MCI_Comp	MCI_OLOF	SII_Comp_LBP	MCI_GCI_ST	CR-based	ECST_A	ECST_M
1	87.16±0.70	83.12±1.08	81.74±0.90	80.99±2.50	90.51±1.43	93.82±0.91	**94.28±0.78**
2	94.90±2.36	93.09±3.70	91.46±3.03	92.09±3.08	95.10±1.44	**98.09±1.45**	**98.07±1.61**
3	96.86±1.68	93.86±3.15	95.19±3.01	95.06±2.09	97.83±1.01	98.84±1.16	**98.96±0.95**
4	98.75±0.18	97.95±0.51	96.48±1.45	97.50±0.55	98.36±0.52	**99.74±0.11**	99.63±0.16
5	99.13±0.19	98.82±0.51	97.89±0.64	98.05±0.54	99.20±0.16	99.70±0.14	**99.75±0.10**
6	99.21±0.18	98.92±0.25	98.21±0.83	98.21±0.77	99.41±0.22	99.79±0.11	**99.81±0.18**

Table III
THE EERS (%) OF PALMPRINT VERIFICATION OBTAINED BY USING DIFFERENT METHODS ON THE POLYU 3D PALMPRINT DATABASE.

Method	EER
MCI_Comp	0.0440
MCI_OLOF	0.0556
SII_Comp_LBP	0.0755
MCI_GCI_ST	0.0928
ECST_A	0.0340
ECST_M	**0.0337**

The comparative results show that the proposed method with using the ECST_A or ECST_M can obtain a higher GAR than other methods against a certain FAR.

Equal Error Rate (EER), which denotes the error rate at the threshold on which both FAR and False Rejection Rate (FRR) are the same, is also employed to evaluate the performance of the proposed method, and compare it with state-of-the-art methods. The EERs obtained by using different methods are presented in Table III, from which we can see that the proposed method with using both the ECST_A and ECST_M perform much better than other methods. In addition, we also see that the ECST_M and ECST_A schemes have very similar ROC curves and EERs, which demonstrates that the Ecomp and cST can be effectively combined by using both the addition and multiplication schemes.

C. Palmprint identification

Palmprint identification is a one-against-many matching process, the task needs to determine the class of a query sample. In this study, we randomly select n palmprint images from each palm as the gallery samples and use the rest as the probe images, and in this paper n is set to 1 to 6, respectively. Given a gallery set, a probe sample is compared with all samples in the gallery set. The class of the gallery sample that produces the maximum matching score, that is the minimum Chi-square distance, with the probe sample is treated as the class of the probe sample. Moreover, the previous published state-of-the-art methods are also implemented and compared them with the proposed method. In each case of gallery set, all algorithms are run for 10 times and the mean identification accurate rates and corresponding standard deviations are reported, as shown in Table IV. It can be seen that the proposed method based on both the ECST_A and ECST_M can achieve higher palmprint identification accuracy than other methods on the PolyU database. Further, the ECST_M performs a litter better than the ECST_M. The possible reason is that the ECST_M effectively consider the association between Ecomp and cST as the same location, and combining them with a label significantly improve the discriminative power of the ECST_M over the Ecomp and cST.

Table V
THE EERS (%) OF PALMPRINT VERIFICATION OBTAINED BASED ON DIFFERENT FEATURES OF 3D PALMPRINT.

Method	EER
Comp	0.0621
Ecomp	0.0390
ST	0.0599
cST	0.0531

D. Comparisons of different features

To evaluate the effectiveness of the Ecomp and cST, we compare them with the competitive code (Comp) and ST based methods in term of verification accuracy, respectively. For fair comparison, we implement these methods with the similar scheme of the ECST_M. Specifically, we form the descriptors of 3D palmprint using the block-wise histograms of the Comp, Ecomp, ST and cST, respectively, and then employ the Chi-square distance in the matching stage. Figure 5 shows the ROC curves obtained by using the Comp, Ecomp, ST and cST based methods, respectively, and the corresponding EERs are listed in Table V. From the comparative experimental

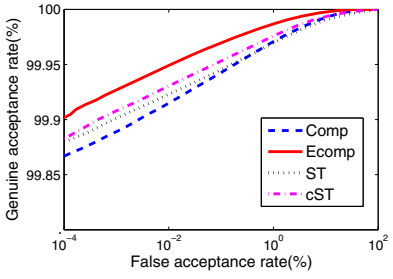

Figure 5. ROC curves obtained by using the competitive code, Ecomp, ST and cST based methods, respectively.

results we can see that the Ecomp performs much better than the competitive code based method. Moreover, it is seen that the cST achieves lower EER than the ST based method. The possible reason is that cST can be accurately and robustly obtained in practical calculation.

Table VI
COMPUTATIONAL TIME COST OF DIFFERENT METHODS.

Method	Feature extraction	Matching
MCI_Comp	62ms	0.63ms
MCI_OLOF	34ms	0.55ms
MCI_GCI_ST	45ms	0.89ms
ECST_A	74ms	0.51ms
ECST_M	76ms	0.50ms

E. Computational complexity analysis

It is widely recognized that the convolution operation is the most time-consuming part of the orientation based method. We see that the proposed method employs the similar Gabor templates as the conventional methods to extract the orientation feature from MCI, so as to has similar computational time cost as them. For better comparison, we compare the computational time cost of the proposed method with that of state-of-the-art methods, including the MCI_Comp, MCI_OLOF, MCI_GCI_ST methods. All algorithms are implemented under MATLAB 8.1.0 platform on a PC with double-core Intel(R) i5-3470 (3.2GHz), RAM 8.00GB, and Windows 7.0 operation system. Further, all algorithms are run for 10 times, and the average time taken in both the feature extraction and matching stages are respectively reported in Table IV. It is seen that the proposed method takes a litter more time than other methods in feature extraction stage. The main reason is that the proposed method extracts extra orientational confidence features of palmprint. The matching time of the proposed method is quit fast for the simple matching scheme. The total time cost of the proposed method is about 85 ms for a one-against-one match, which is acceptable in a real-world application.

V. CONCLUSION

In this paper, a novel enhanced competitive code is developed to represent both the orientation features and the corresponding orientational confidence of 3D palmprint, and a simple and effective compact-ST is employed to improve the robustness of 3D palmprint surface representation. Further, the Ecomp and cST can be effectively fused using the addition and multiplication strategies to better represent both the 2D orientation and 3D surface shape features of the 3D palmprint. Experimental results have shown the effectiveness of the proposed method on both 3D palmprint verification and identification.

ACKNOWLEDGMENT

This paper is partially supported by the National Natural Science Foundation of China (No. 61702110), and the Guangdong Province high-level personnel of special support program (No. 2016TX03X164).

REFERENCES

[1] J. Dai, J. Feng, and J. Zhou, "Robust and efficient ridge-based palmprint matching," IEEE Trans. Pattern Analysis and Machine Intelligence, vol.34, pp.1618–1632, 2012.

[2] L. Fei, Y. Xu, W. Tang, and D. Zhang, "Double-orientation code and nonlinear matching scheme for palmprint recognition," Pattern Recognition, vol.49, pp.89–101, 2016.

[3] A. Kong, D. Zhang, and M. Kamel, "A survey of palmprint recognition," Pattern Recognition, vol.42, pp.1408–1418, 2009.

[4] D. Zhang, W. K. Kong, J. You, and L. M. Wong, "Online palmprint identification," IEEE Trans. Pattern Analysis and Machine Intelligence, vol.25, pp.1041–1050, 2003.

[5] L. Fei, B. Zhang, Y. Xu, and L. Yan, "Palmprint Recognition Using Neighboring Direction Indicator," IEEE Trans. Human-Machine Systems, vol.46, pp.787–798, 2016.

[6] X. Wu, Q. Zhao and W. Bu, "A sift-based contactless palmprint verification approach using iterative ransac and local palmprint descriptors", Pattern recognition, vol.47, pp.3314–3326, 2014.

[7] A. K. Jain and J. Feng, "Latent palmprint matching," IEEE Trans. Pattern Analysis and Machine Intelligence, vol.30, pp.1032–1047, 2009.

[8] E. Liu, A. K. Jain, and J. Tian, "A coarse to fine minutiae based latent palmprint matching," IEEE Trans. Pattern Analysis and Machine Intelligence, vol.35, pp.2307–2322, 2013.

[9] D. Zhang, G. Lu, W. Li, L. Zhang, and N. Luo, "Palmprint recognition using 3d information," IEEE Trans. System, Man, and Cybernetics, Part C: Applications and Reviews, vol.39(5), pp.505–519, 2009.

[10] D. Zhang, G. Lu, W. Li, L. Zhang, and N. Luo, "Three dimensional palmprint recognition using structured light imaging," Proc. IEEE International Conference on Biometrics: Theory, Applications and Systems, 2008, pp.1–6.

[11] W. Li, D. Zhang, L. Zhang, G. Lu, and J. Yan, "3-d palmprint recognition with joint line and orientation features," IEEE Trans. System, Man, and Cybernetics, Part C: Applications and Reviews, vol.41, pp.274–279, 2011.

[12] W. Li, L. Zhang, and D. Zhang, "Three dimensional palmprint recognition," Proc. IEEE International Conference on Systems, Man, and Cybernetics, 2009, pp.4847–4852.

[13] B. Yang, X. Wang, J. Yao, and X. Yang, "Efficient local representation for three-dimensional palmprint recognition," Journal of Electronic Imaging, vol.22, pp.043040C1–043040C9, 2013.

[14] L. Zhang, Y. Shen, H. Li, and J. Lu, "3d palmprint identification using block-wise features and collaborative representation," IEEE Trans. Pattern Analysis and Machine Intelligence, vol.37, pp.1730–1736, 2015.

[15] G. Hetzel, B. Leibe, P. Levi, and B. Schiele, "3d object recognition from range images using local feature histograms," Proc. IEEE Conference on Computer Vision and Pattern Recognition (CVPR), 2011, pp.394–399.

[16] M. Liu and L. Li, "Cross-correlation based binary image registration for 3d palmprint recognition," Proc. IEEE International Conference on Signal Processing (ICSP), 2012, pp.1597–1600.